Electronic Supplementary Information for Dalton Transactions

Supplementary Information for

Photoinduced energy transfer in multichromophores based on planar Pt-bipyridine-acetylide and octahedral Ru-bipyridine centres

Raymond Ziessel,*[a] Julie Batcha Seneclauze,[a] Barbara Ventura,[b] Andrea Barbieri,[b] and Francesco Barigelletti*[b]

Purification and characterization of the complexes.

All compounds were systematically purified by column chromatography on alumina as solid phase and CH_2Cl_2/CH_3OH as mobile phase. Recrystallization in adequate solvents afforded the analytically pure samples. Selected data for **Pt**: ESI-MS (CH_3CN) *m/z* 822.3 ($[M+H]^+$, 100); FT-IR 2109.7 cm^{-1} ($\nu_{C\equiv C}$); elemental analysis Found: C, 61.19, H, 4.42, N, 10.02. $C_{42}H_{38}N_6Pt$ requires: C, 61.38; H, 4.66; N, 10.23; for **PtRu**: ESI-MS (CH_3CN) *m/z* 1380.2 ($[M-PF_6]^+$, 100), 617.5 ($[M-2PF_6]^{2+}$, 40); FT-IR 2109.3 cm^{-1} ($\nu_{C\equiv C}$); elemental analysis C, 48.52, H, 3.23, N, 8.87. $C_{62}H_{54}F_{12}N_{10}P_2PtRu$ requires C, 48.82; H, 3.57; N, 9.18. ^1H NMR in d_6-acetone δ 9.58 (1H, d, ^3J = 6.8 Hz), 9.36 (1H, d, ^3J = 6.0 Hz), 8.86-8.79 (4H, 4 line m), 8.73 (1H, d, ^3J = 8.5 Hz), 8.67-8.66 (4H, 2 line m), 8.57 (1H, s), 8.49 (1H, d, ^3J = 7.6 Hz), 8.42 (1H, d, ^3J = 8.0 Hz), 8.23-8.11 (8H, 8 line m,), 8.05 (1H, d, ^3J = 5.0 Hz), 8.01-7.93 (4H, 8 line m), 7.82-7.79 (3H, 5 line m), 7.63-7.50 (5H, 9 line m), 7.41 (1H, t, ^3J = 6.6 Hz), 1.46 ppm (18H, s,).for **$PtRu_2$**: ESI-MS (CH_3CN) *m/z* 2083.2 ($[M-PF_6]^+$, 100), 969.0 ($[M-2PF_6]^{2+}$, 80); 598.1 ($[M-3PF_6]^{3+}$, 50); FT-IR 2114.4 cm^{-1} ($\nu_{C\equiv C}$); elemental analysis C, 43.78, H, 2.93, N, 8.49. $C_{82}H_{70}F_{24}N_{14}P_4PtRu_2$ requires: C, 44.19; H, 3.17; N, 8.80. ^1H NMR in d_6-acetone δ 9.18 (2H, d, ^3J = 5.8 Hz), 8.84-8.69 (13H, 11 line m), 8.21-7.98 (22H, 13 line m), 7.84 (2H, s), 7.72-7.50 (13H, 12 line m), 1.46 ppm (18H, s).

Electrochemistry.

With reference to the Table below, to notice the following.

1) The oxidation on the **PtRu** and **$PtRu_2$** complexes is Ru based due to the clear reversibility compared to the irreversible oxidation of the **Pt** precursor at higher potential.

2) The first reduction on the **PtRu** and **$PtRu_2$** complexes is based on the Ru part, i.e., on the ethynylbpy ligand. A second very close reversible reduction is likely localized on the Pt part, the third reduction is localized on the Ru-unsubstituted bpy.

3) The third reduction of the unsubstituted bpy is not observed, as usually for $[Ru(bpy)_3]^{2+}$, or the Ru complex which has a second two electron reduction wave.

Table . Electrochemical data for the Pt/Ru complexes.[a]

Cmpds	$E^{0'}$(ox, soln) (V), ΔE (mV)	$E^{0'}$(red, soln) (V), ΔE (mV)
Pt	+1.37 (irrev, Ia/Ic ≈ 0)	-1.43 (70)
Pt(bpy)Cl_2	+1.38 (irrev, Ia/Ic ≈ 0)	-1.38 (80)
PtRu	+1.32 (70)*	-1.33 (60), -1.38 (70), -1.61 (60)
$PtRu_2$	+1.32 (70)*	-1.34 (60), -1.39 (60), -1.63 (60)
Ru	+1.40 (60)	-1.17 (60), -1.55 (100)**

[a]Potentials determined by cyclic voltammetry in deoxygenated CH_3CN solution, containing 0.1 M $TBAPF_6$, at a solute concentration of ca. 1.5 mM and at rt. Potentials were standardized versus ferrocene (Fc) as internal reference and converted to the SCE scale assuming that $E_{1/2}$ (Fc/Fc^+) = +0.38 V (ΔEp = 60 mV) *vs* SCE. Error in half-wave potentials is ±15 mV, all potential correspond to single electron transfer processes unless otherwise noticed. For irreversible processes the peak potentials (E_{ap} or E_{cp}) are quoted. (*) The visibility is perturbed by adsorption of the complex on the electrolyte surface. (**) Two-electron process.

Pt→Ru energy transfer in PtRu and $PtRu_2$

From the luminescence properties of Pt and Ru, **Pt→Ru** energy transfer is exothermic by *ca*. 0.4 eV. For **PtRu** and **$PtRu_2$**, the electronic interaction between the partners is likely weak, as suggested by the fact that the Ru-based unit largely keeps its individual electronic properties in the MLCT absorption region. On this basis, we tentatively discard the dual electron exchange (i.e., through-bond) Dexter energy transfer. [1] For the dipole-dipole Förster mechanism, [2] evaluation of the spectral overlap J_F between the luminescence profile of **Pt** and the absorption profile of bound **Ru** (which overlaps that of the Ru-based unit in **PtRu,** Figure 1 of main text), allows the estimate of the **Pt→Ru** energy transfer rate constant, k_{en}^{F}, at an intermetal separation d_{cc} ≅. 9 Å, eqs. 1-3,

$$J_F = \frac{\int F(\bar{\upsilon})\varepsilon(\bar{\upsilon})/\bar{\upsilon}^4 d\bar{\upsilon}}{\int F(\bar{\upsilon})} \quad (1)$$

$$k_{en}{}^{F} = \frac{8.8\times10^{-25} K^2 \phi_{em}}{n^4 \tau_{em} d_{cc}{}^{6}} J_F \quad (2)$$

$$R_o(\text{Å}) = 9.79\times10^3 \left(K^2 n^{-4} \phi_{em} J_F\right)^{1/6} \quad (3)$$

where F($\bar{\nu}$) and ε($\bar{\nu}$) are the luminescence and absorption profiles on an energy scale (cm^{-1}) of **Pt** and **Ru**, respectively, K^2 is a geometric factor (taken as 2/3); ϕ_{em} and τ_{em} are the luminescence quantum yield and lifetime, respectively, of **Pt** (the excitation energy donor), n is the refractive index of the solvent, the intermetal distance d_{cc} is estimated 9 Å from molecular modeling, and R_o is the critical transfer radius. Results were $J_F = 8.2 \times 10^{-15}$ cm^3 M^{-1}, $k_{en}{}^F = 1.04 \times 10^8$ s^{-1} (at 9 Å), and R_o = 25.2 Å. Figure SI_1 provides a schematic layout for the Pt- and Ru-based energy levels involved.

SI References

1 D. L. Dexter, *J. Chem. Phys.*, 1953, 21, 836.

2 T. Förster, *Discuss. Faraday Soc.*, 1959, 27, 7.

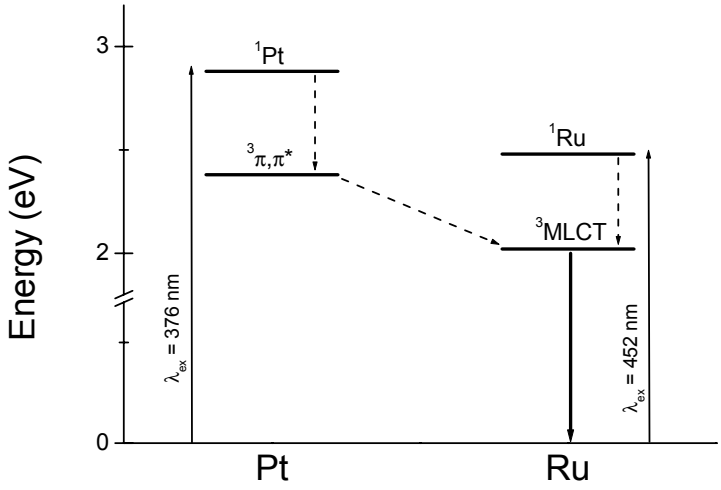

Figure SI_1. Energy layout for the Pt- and Ru-based levels in **PtRu** and **PtRu$_2$**. ILCT levels are not indicated.